Universitat de les Illes Balears
IAC3 Institut d'Aplicacions Computacionals de Codi Comunitari

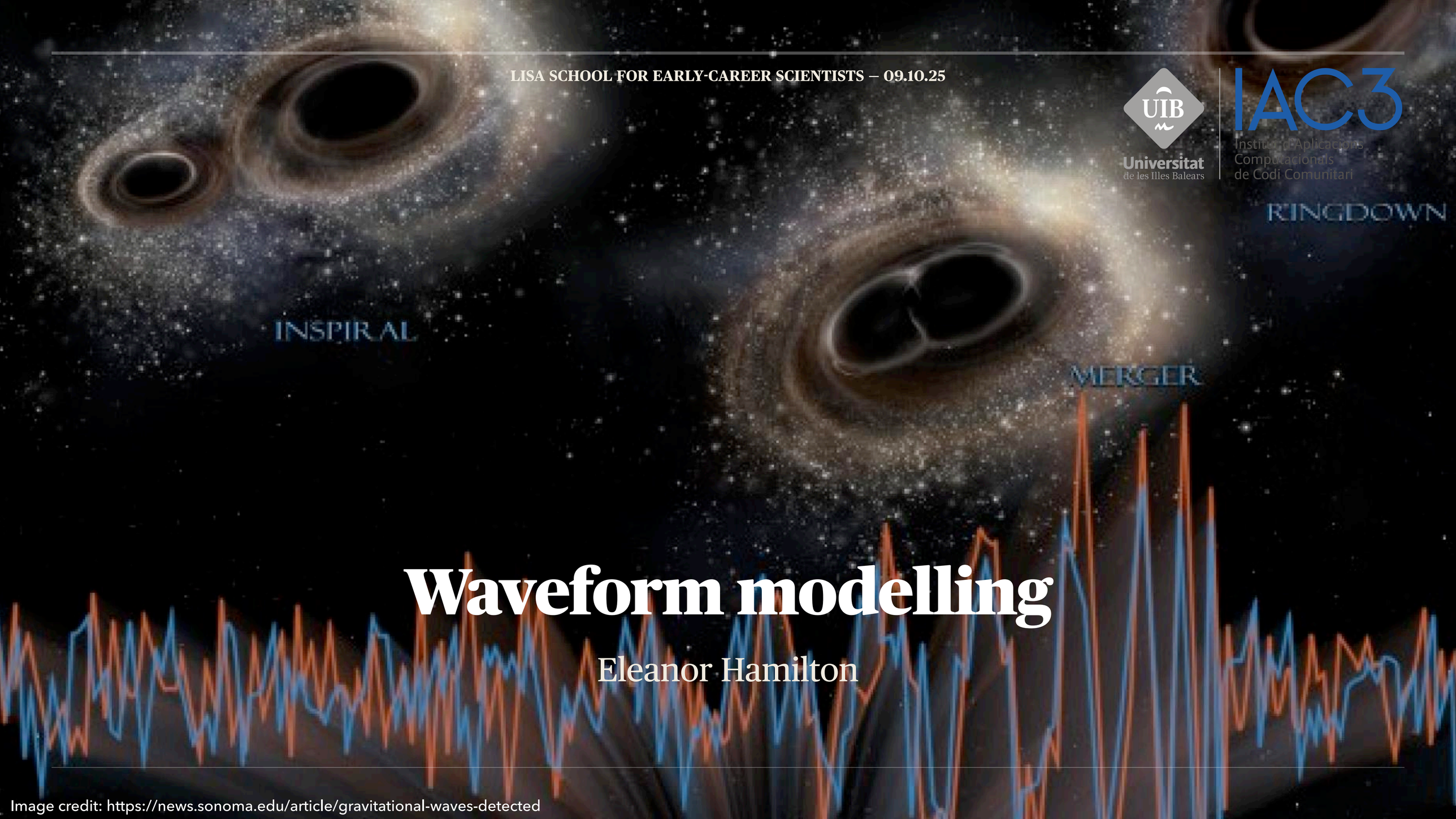

Waveform modelling

Eleanor Hamilton

Image credit: https://news.sonoma.edu/article/gravitational-waves-detected

LISA SCHOOL FOR EARLY CAREER SCIENTISTS – 09.10.25

Modelling approaches

For different sources

LISA sources

- Main sources for LISA:
  - Massive Black Hole Binaries (MBHBs)
  - Galactic binaries
  - Extreme Mass Ratio Inspirals

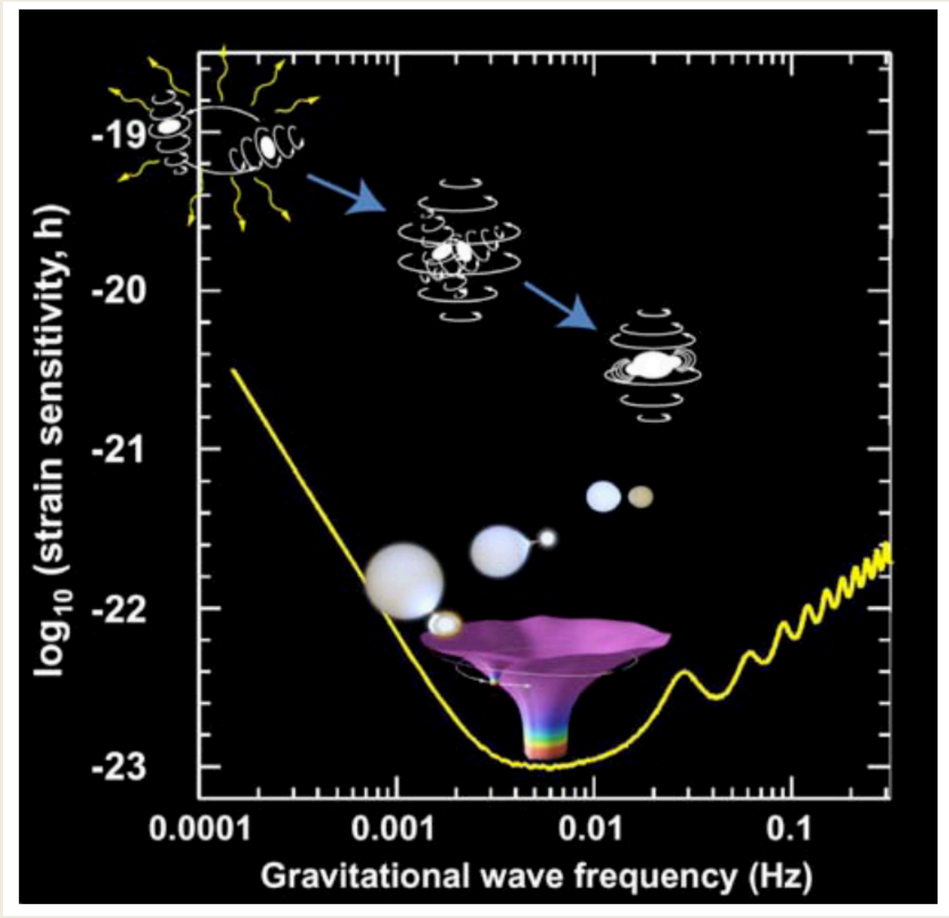

LISA-LIST team. LISA: Probing the universe with gravitational waves. Technical report, LISA Mission Science Office, 2007.

Modelling approaches

- 3 main approaches to resolving the spacetime around radiating binaries:
  - Numerical relativity
  - post-Newtonian/post-Minkowskian theory
  - Gravitational self-force
- Effective formulations to cover larger regions of parameter space:
  - Effective-one-body
  - Phenom

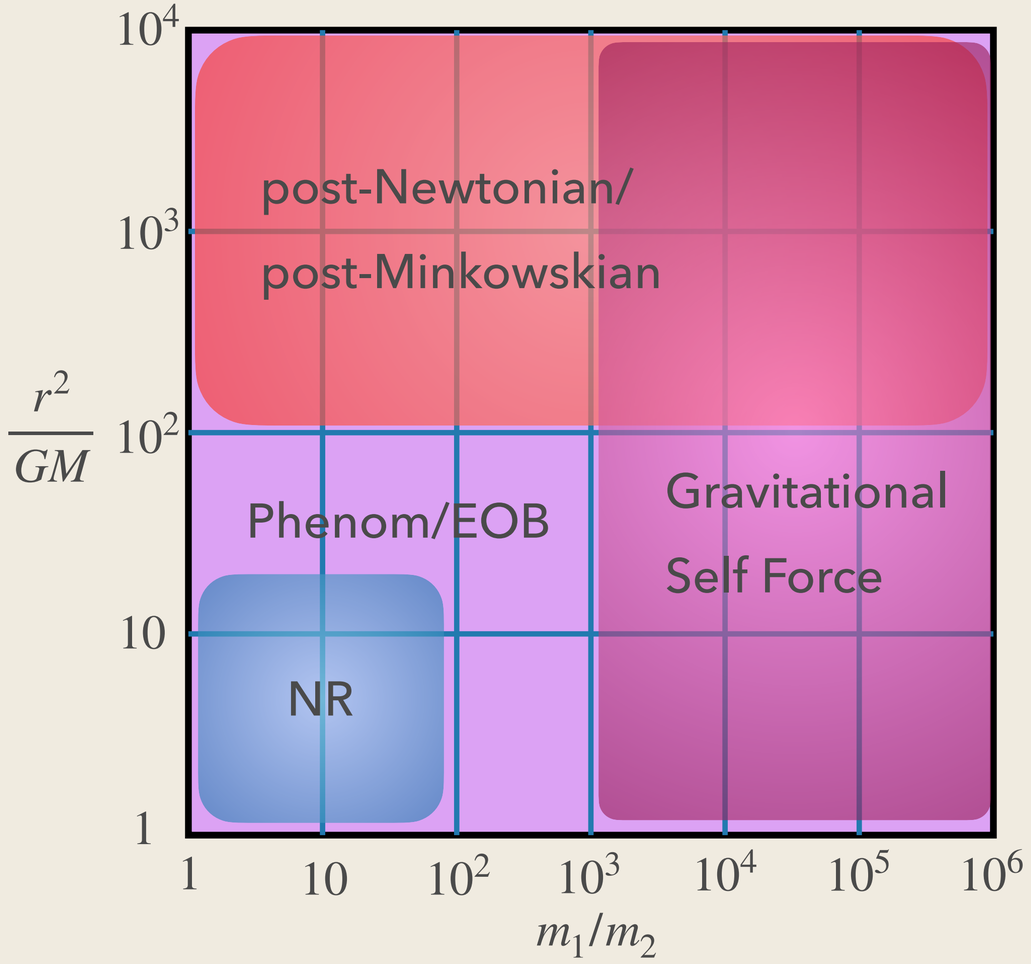

Physical Phenomena

- Non-spinning/aligned-spin systems
- Arbitrarily oriented spins
- Asymmetric masses
- Eccentric orbits
- Fully generic binaries

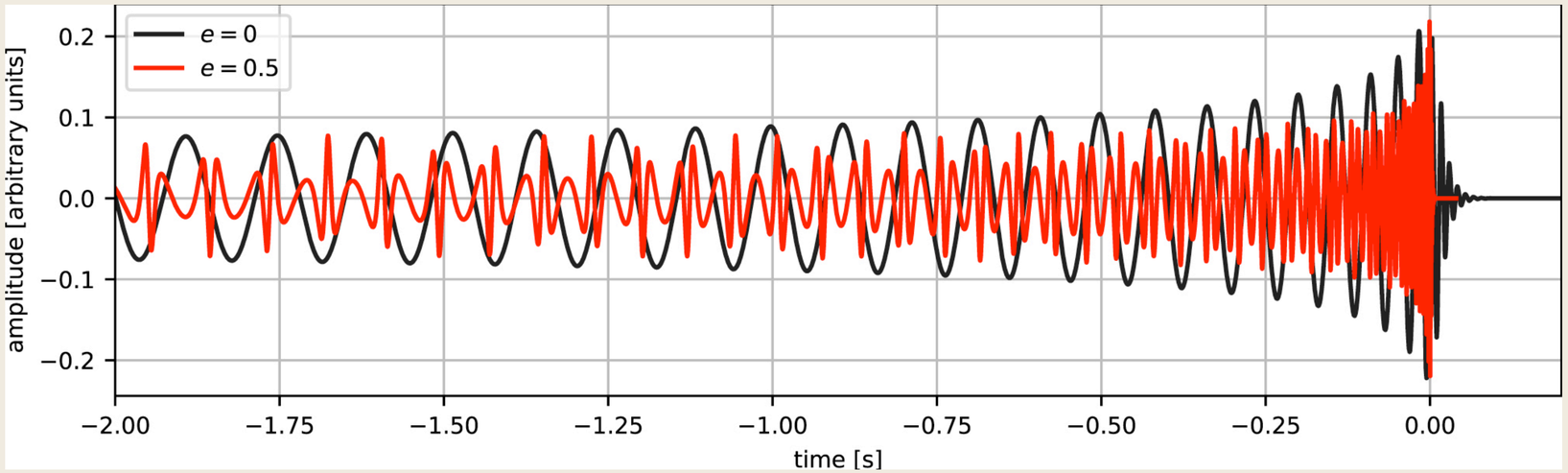

Abbott, B. P., et al. "Search for eccentric binary black hole mergers with Advanced LIGO and Advanced Virgo during their first and second observing runs." The Astrophysical Journal 883.2 (2019): 149.

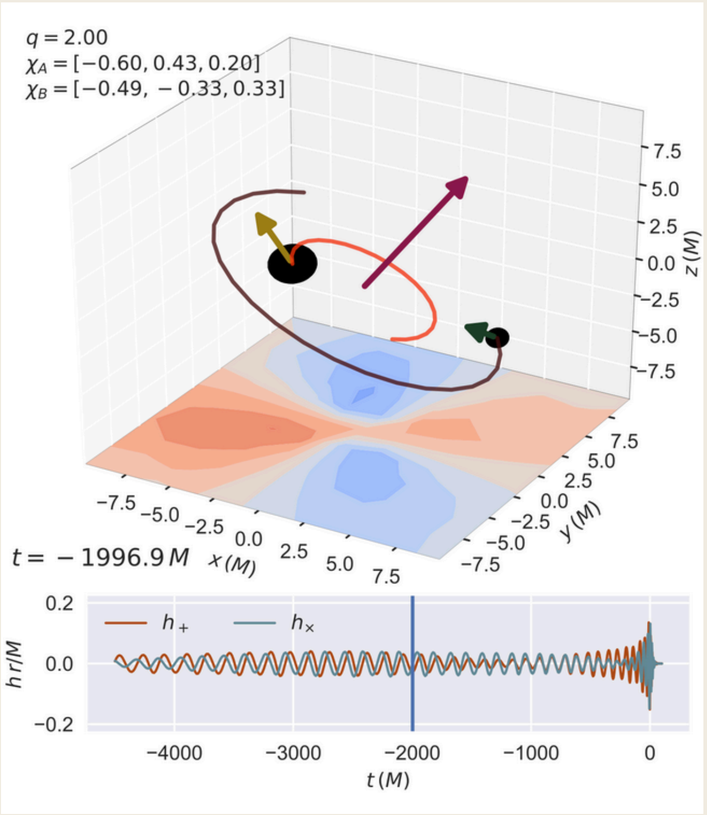

Varma, Vijay, Leo C. Stein, and Davide Gerosa. "The binary black hole explorer: on-the-fly visualizations of precessing binary black holes." Classical and Quantum Gravity 36.9 (2019): 095007.

Effective-One-Body formalism

- Maps two-body dynamics onto that of an effective test mass/spin in a deformed Schwarzschild/ Kerr background

1. Produce **Hamiltonian** describing **conservative** dynamics

   $$H_{\mathrm{EOB}} = M\sqrt{1 + 2\nu\left(\frac{H_{\mathrm{eff}}}{\mu} - 1\right)}$$

   for an effective Hamiltonian H_{eff} of a test mass μ moving in a Kerr spacetime of mass M deformed by amount ν

2. Introduce **radiation-reaction**

Effective-One-Body: SEOB

- Combines information from analytical methods with numerical relativity data
- Includes:
  - Tidal and generic spin interactions
  - Generic orbits
- Suitable for IMRIs/MBHBs

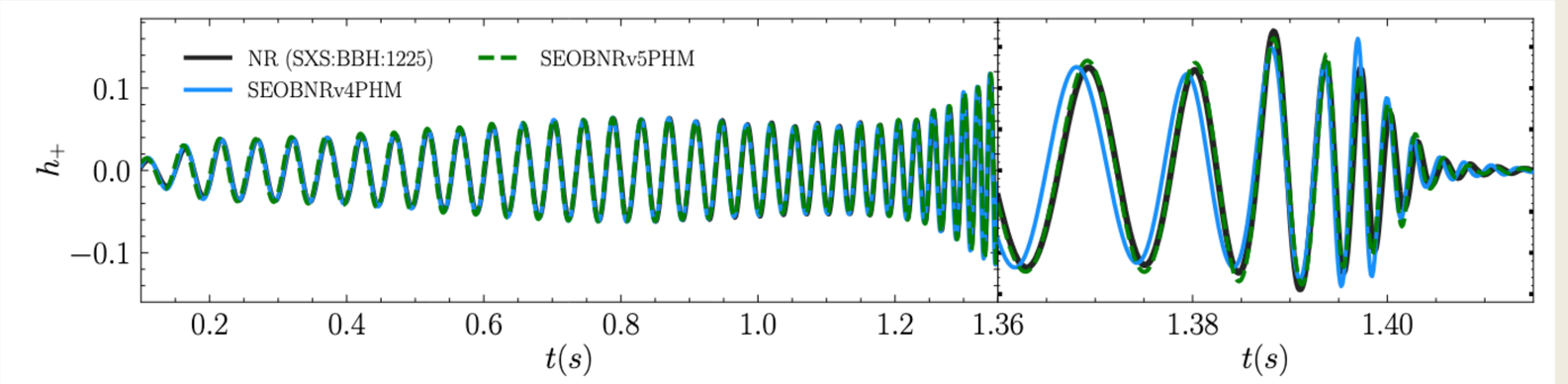

Ramos-Buades, Antoni, et al. "Next generation of accurate and efficient multipolar precessing-spin effective-one-body waveforms for binary black holes." Physical Review D 108.12 (2023): 124037.

Effective-One-Body: TEOB

- Includes systematic resumption of EOB potentials via Padé approximants
- Includes:
  - Tidal and generic spin interactions
  - Generic orbits (arbitrary eccentricity, hyperbolic, scattering)
  - Gravitational self-force
- Minimal NR calibration

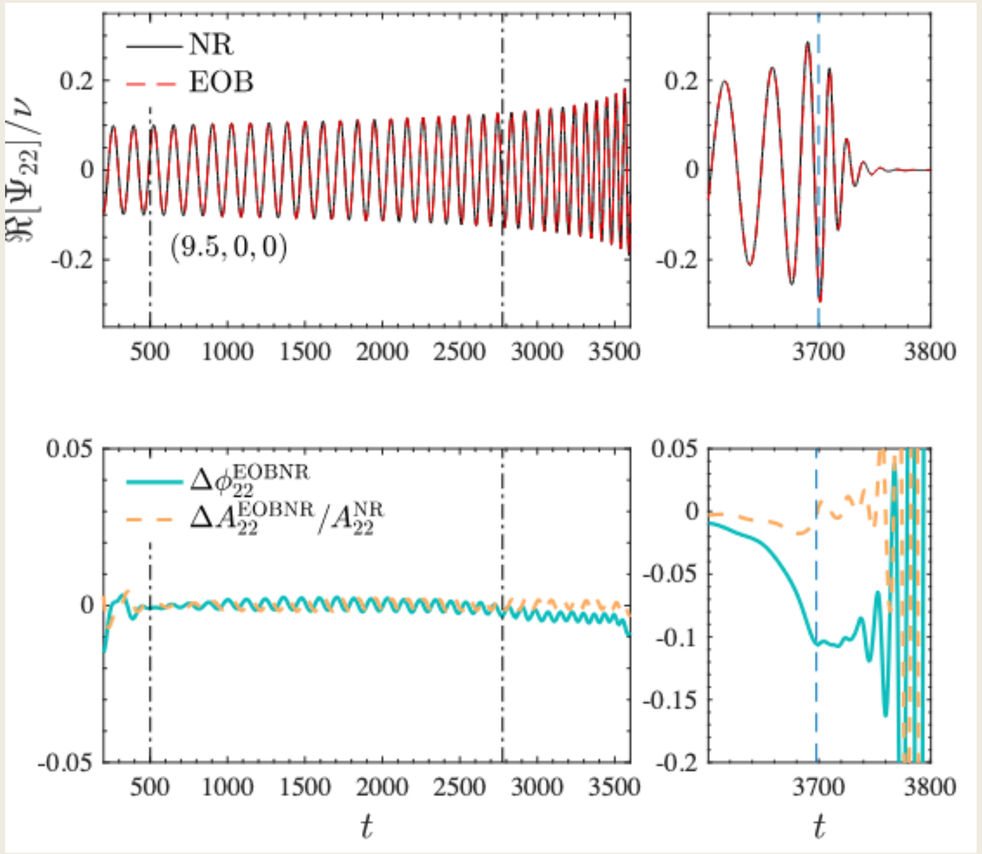

Nagar, Alessandro, et al. "Analytic systematics in next generation of effective-one-body gravitational waveform models for future observations." Physical Review D 108.12 (2023): 124018.

Phenomenological models

- Complete IMR model; evaluates down to arbitrary frequencies
- Largely relies on closed-form expressions to ensure efficiency
- Construction of model:
  - Appropriate piece-wise ansatz
  - Fit co-efficients to calibration data set
  - Co-efficients interpolated across parameter space
- Suitable for MBHBs/IMRIs

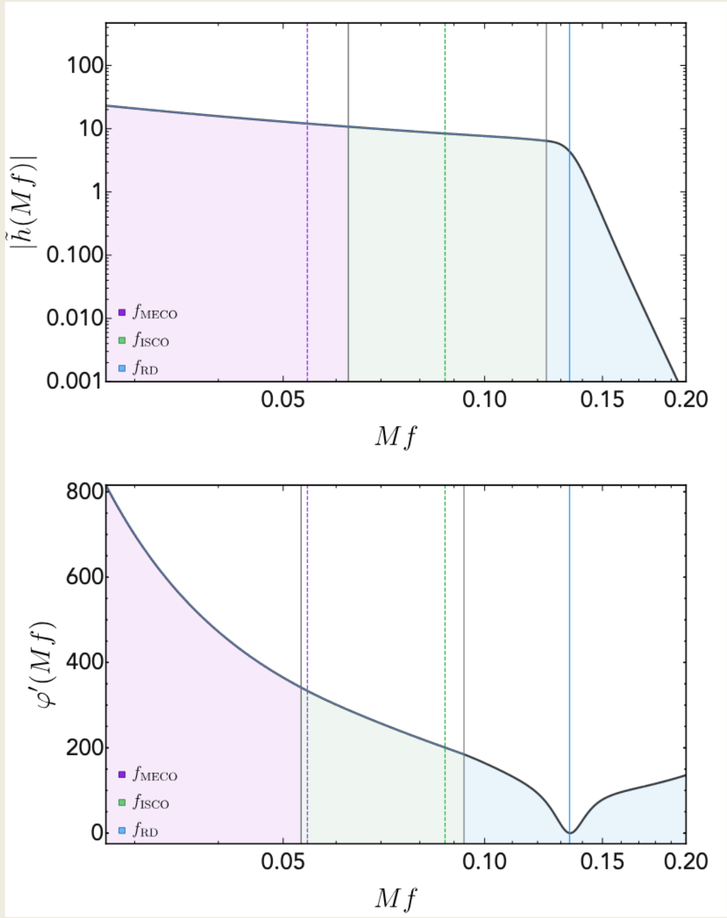

Pratten, G, et al. Physical Review D 102.6 (2020): 064001.

Surrogate models

- A **data driven** approach
- Interpolates large data sets with no assumptions about the phenomenology of the underlying waveforms
  - **Accurate**
  - **Finite length**
- Range of available models:
  - NRSur7dq4 (MBHBs)
  - BHPTNRSurrogate (MBHB/IMRI)

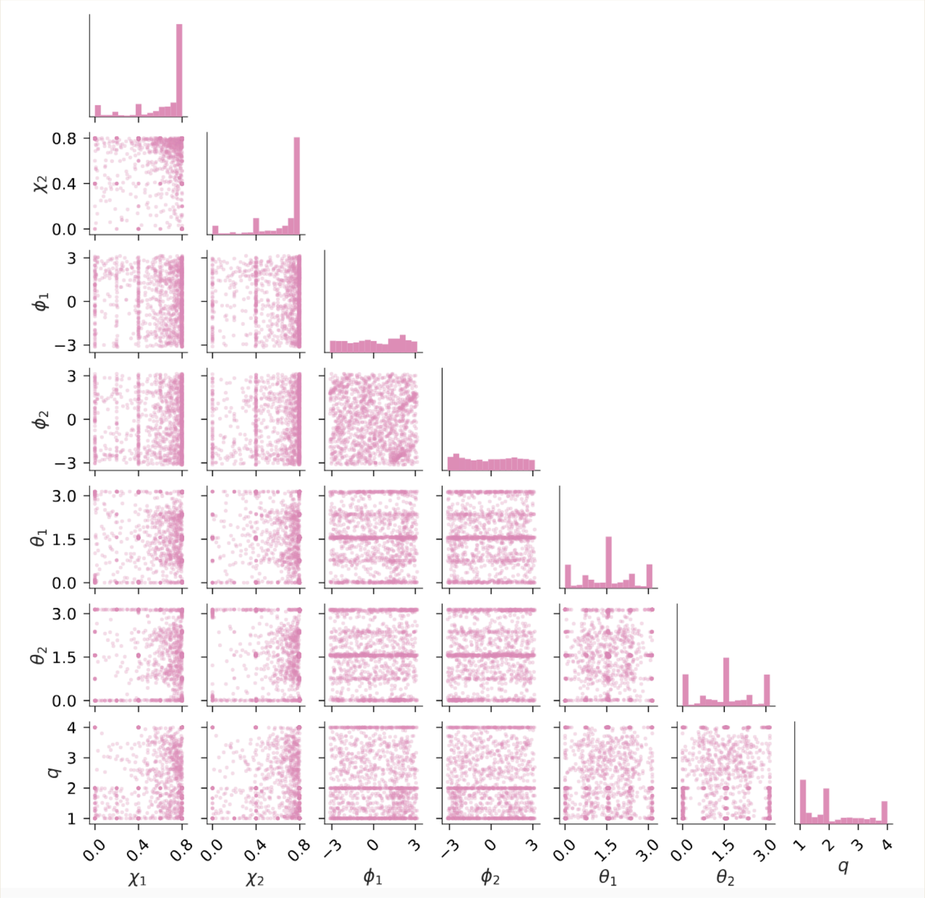

Varma, V., et al. "Surrogate models for precessing binary black hole simulations with unequal masses." Phys Rev Research 1.3 (2019): 033015.

LISA SCHOOL FOR EARLY CAREER SCIENTISTS – 09.10.25

Modelling requirements

From data analysis

Requirements

- Ideal:
  - Infinitely accurate
  - Highly computationally efficient
- Errors in models:
  - Hamper detection and identification of sources
  - Affect tests of GR, rate and population estimates, formation models…
  - Introduce residuals when subtracting sources

Accuracy measures

- Can look at dephasing, errors in the fits, etc.

- When using waveforms, the more interesting quantity when assessing accuracy is the match

$$M(h_1, h_2) = \max\left[4\mathrm{Re}\int \frac{h_1(f)h_2^*(f)}{S_n(f)}\mathrm{d}f\right]$$

$$\mathscr{M} = 1 - M(h_1, h_2)$$

- Ideally, all models would include a measure of their error across the parameter space

- Need to understand how traditional accuracy measure relate to bias in parameter estimation

Accuracy measures and biasses

- Ideally, all models would include a measure of their error across the parameter space

- Need to understand how traditional accuracy measure relate to bias in parameter estimation
  e.g. distinguishability criterion

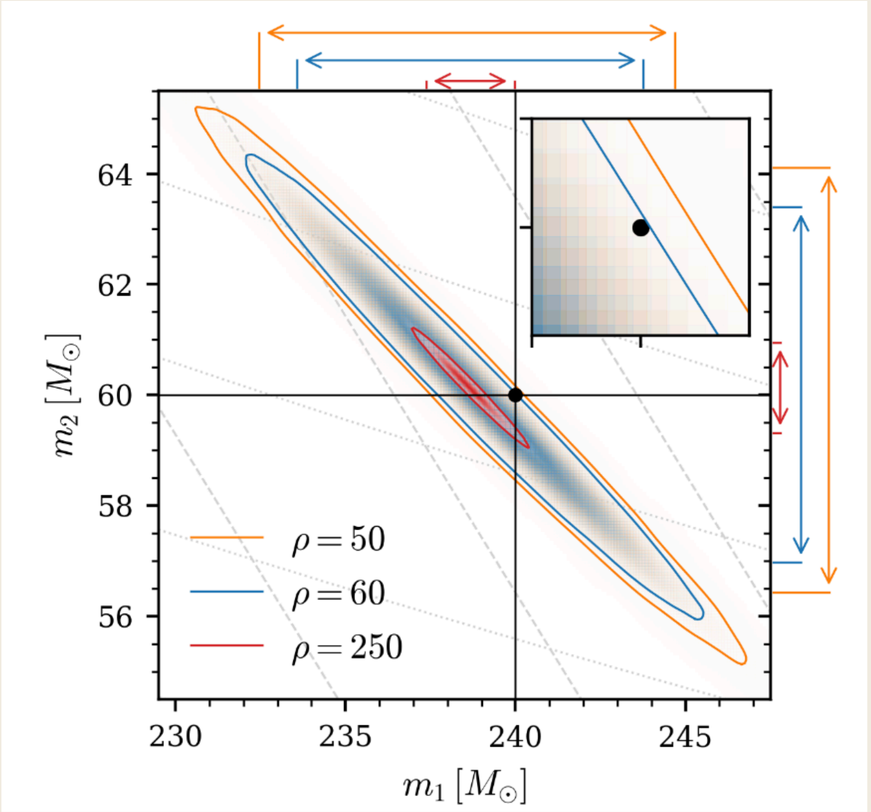

Thompson, Jonathan E., et al. "Use and interpretation of signal-model indistinguishability measures for gravitational-wave astronomy." Physical Review D 112.6 (2025): 064011.

LISA SCHOOL FOR EARLY CAREER SCIENTISTS – 09.10.25

Case study:

Creating a phenomenological precessing model

Precessing systems

- A **precessing** binary is one where the spin on one or both of the black holes is mis-aligned with the orbital angular momentum

- This introduces **oscillations** in the amplitude and phase of the waveform, making it harder to model

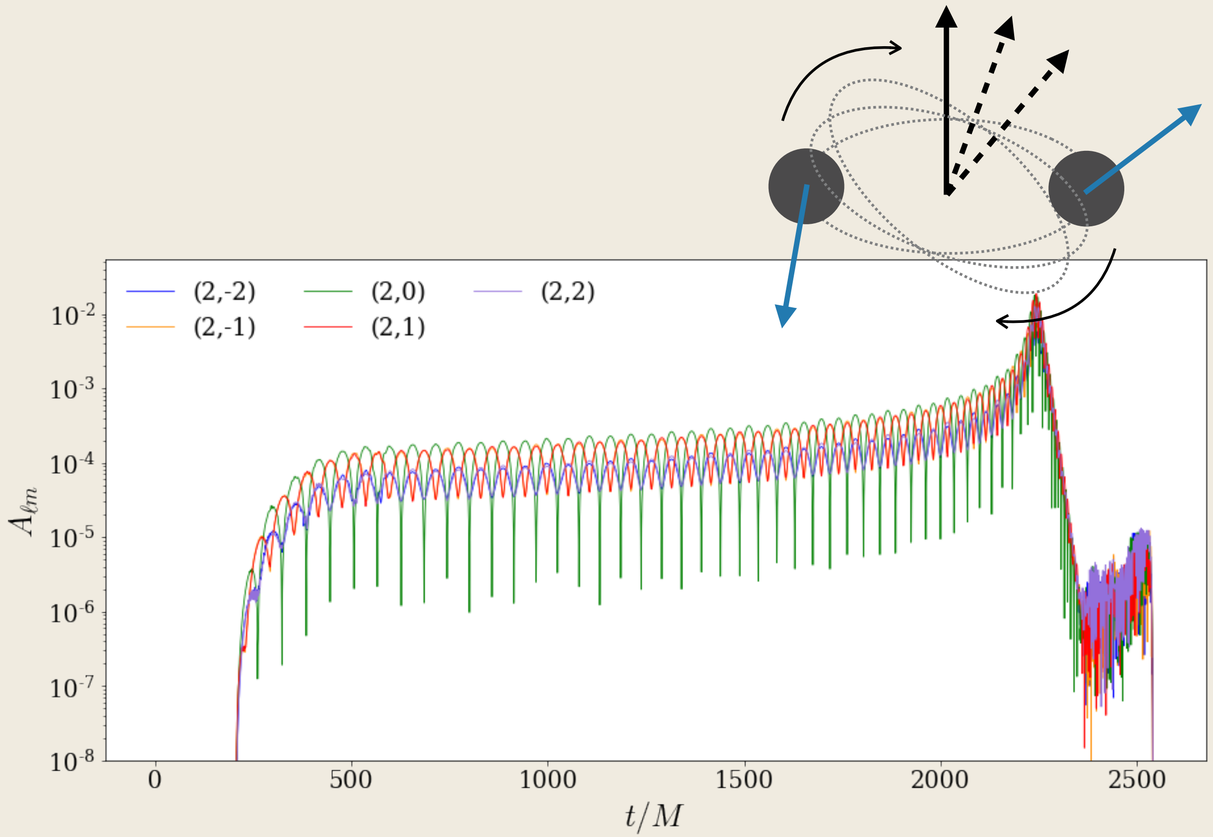

Inertial frame (with J ∥ z) waveform

Modelling precessing systems

- To simplify the modelling of a precessing system, we use the **co-precessing frame**, where the waveform resembles a non-precessing one
- We now need to model the **co-precessing waveform** and the **precession dynamics**

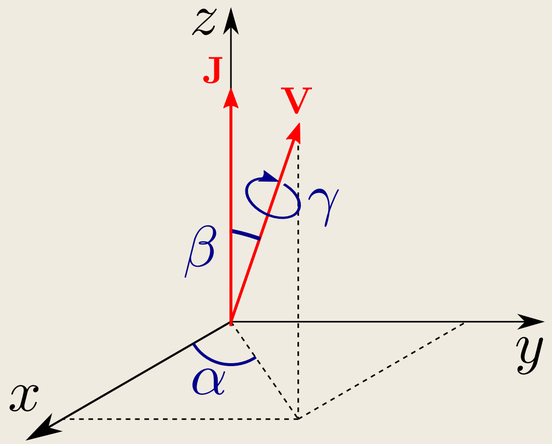

Representation of the three precession angles. V indicates the optimal emission direction (or the orbital angular momentum)

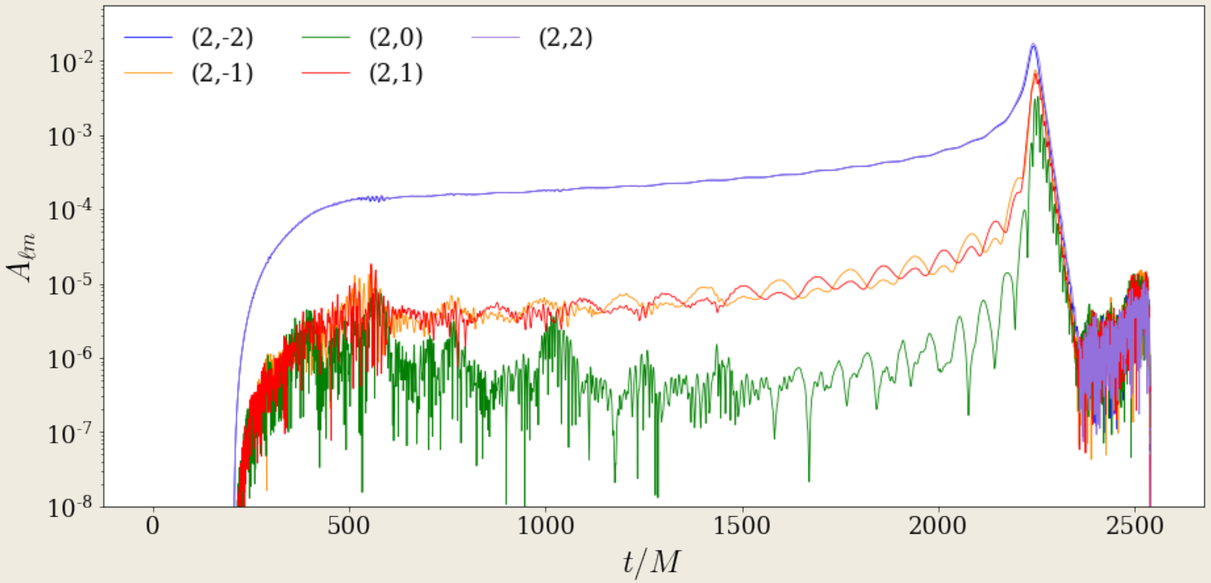

Co-precessing frame waveform

Co-precessing waveform

- **Co-precessing model**
  - Based on PhenomXAS
    - Calibrated to hybrid EOB + NR hybrids
    - Employs PN TaylorF2 in inspiral with pseudo-PN terms calibrated to hybrid data
    - Phenomenological merger-ringdown
    - Connected via colocation points

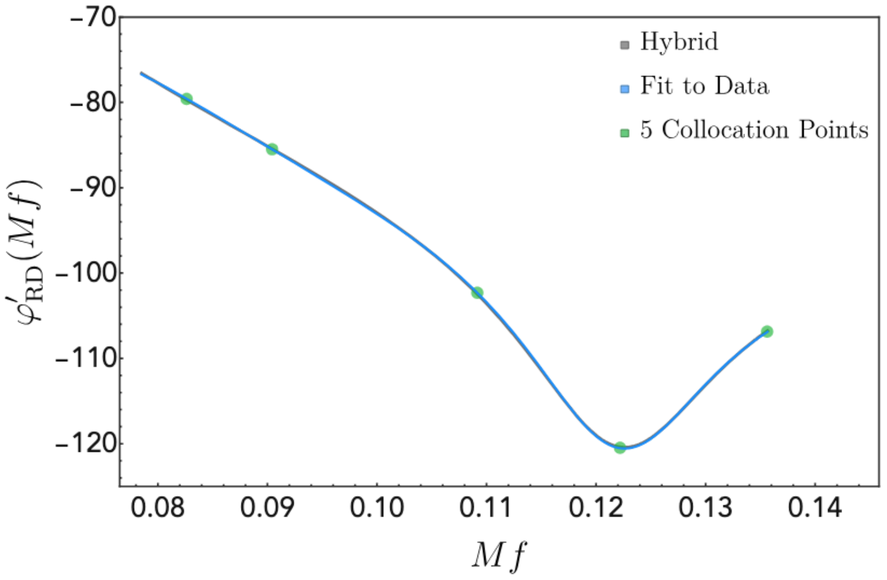

FIG. 10. Phase derivative for SXS-BBH-0153 hybridized against SEOBNRv4 in the merger-ringdown region along with the fit to the data (blue) reconstructed from a system of collocation points (green).

Pratten, Geraint, et al. "Setting the cornerstone for a family of models for gravitational waves from compact binaries: The dominant harmonic for nonprecessing quasicircular black holes." Physical Review D 102.6 (2020): 064001.

Co-precessing waveform

- **Co-precessing model**
  - Tuned parameters in merger-ringdown ansatz to precessing simulations
  - Key feature: effective ringdown frequency
  - Includes calibrated multipole asymmetry

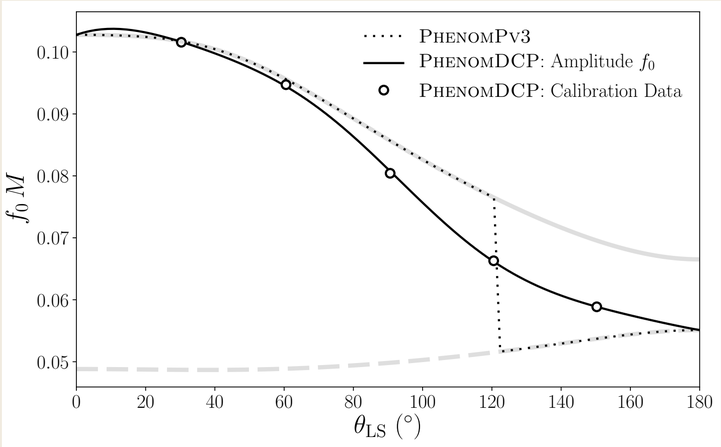

Evolution of the ringdown frequency across the parameter space for cases with mass ratio 8, dimensionless spin 0.8

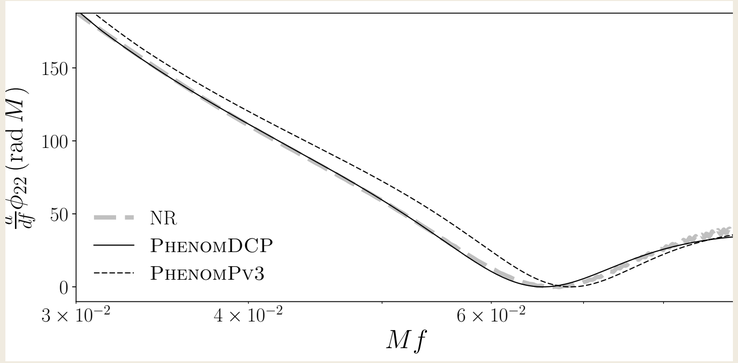

Phase derivative

Dominant multipole precession dynamics

- **Precession angle model**
  - Use SpinTaylor PN expressions for angles in inspiral
  - Phenomenological ansatz describes merger-ringdown behaviour
  - Captures key physical features
    - Ringdown value of β
    - Mode hierarchy
  - γ calculated using minimal rotation condition

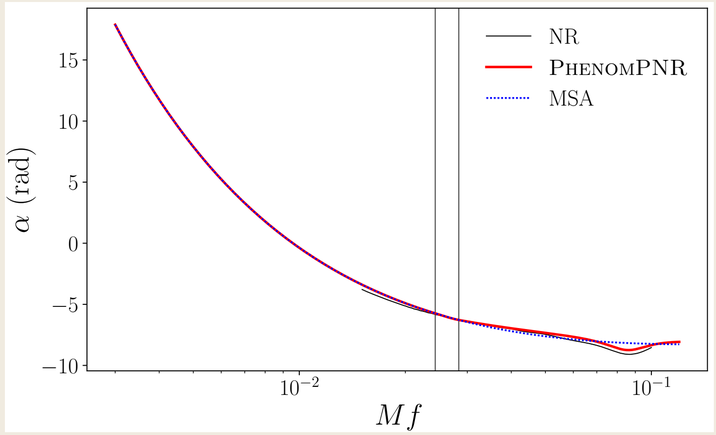

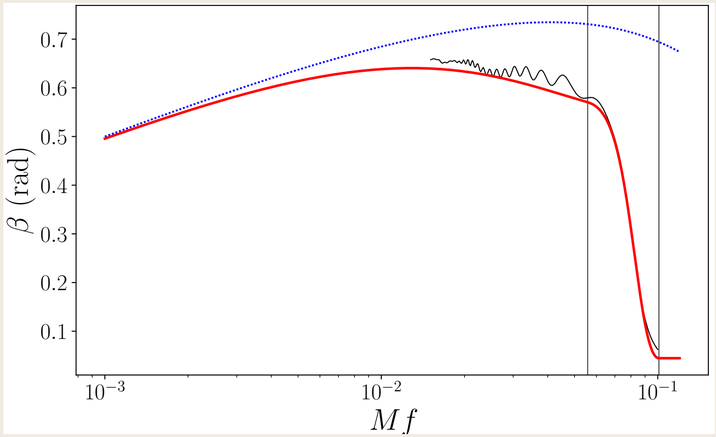

Collapse of β through merger

- β drops rapidly during merger
- Inspiral can be described by PN theory and ringdown can be described by perturbation theory
- Drop itself cannot be described by either theory

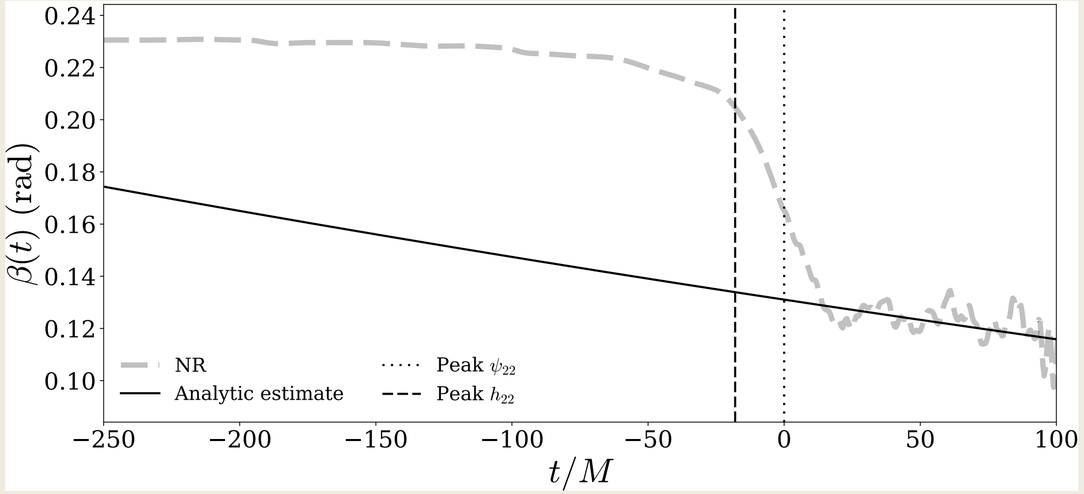

$q = 8, \chi = 0.4, \theta_{LS} = 30^\circ$

Mode hierarchy

- In precessing waveforms we see a hierarchy in the turnover frequency of precessing waveforms
- This is related to the rapid drop off in beta since

$$\beta = 2 \arctan \frac{|h^J_{21}|}{|2h^J_{22}|}$$

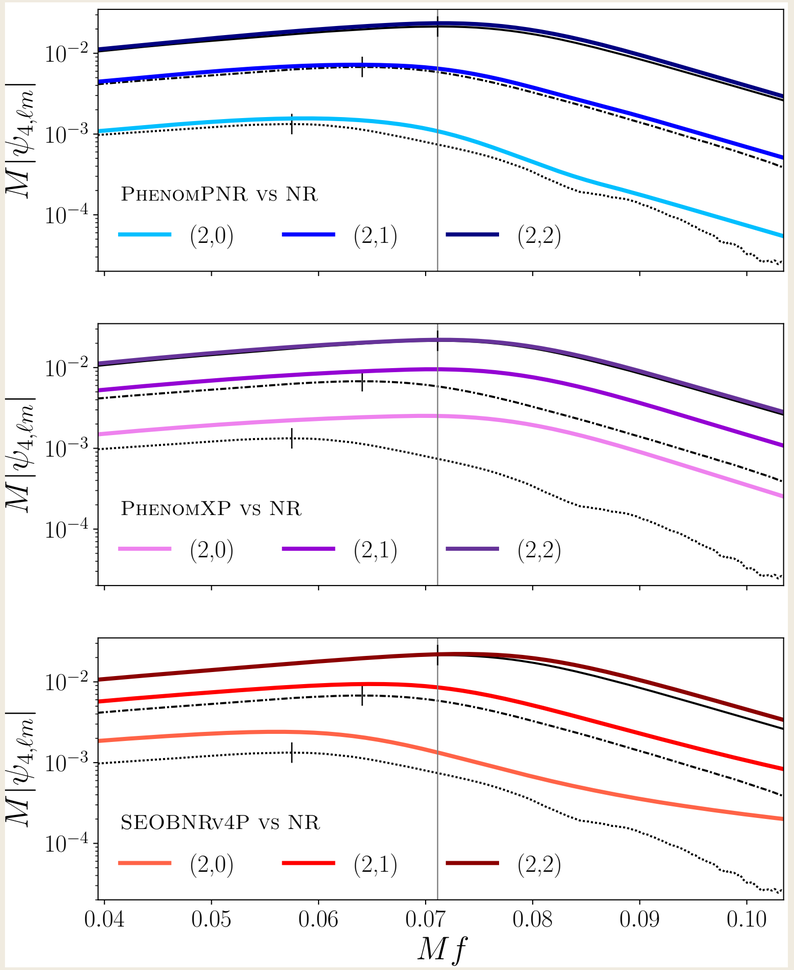

Ringdown frequency

- The remnant black hole formed after a binary-black-hole merger emits gravitational waves at characteristic frequencies, known as quasi-normal modes (QNMs)
- Frequencies determined by perturbation theory but amplitudes unknown
- For each QNM we have both a prograde and a retrograde frequency
- Basic picture: if the perturbation is in the same direction as the final spin, prograde frequencies are excited and vice versa, where the perturbation is in the same direction as orbital direction

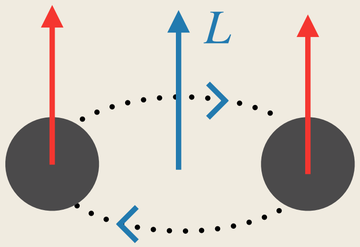

Initial binary

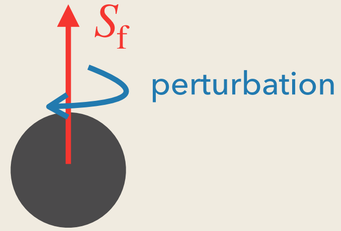

Remnant

Prograde frequencies excited

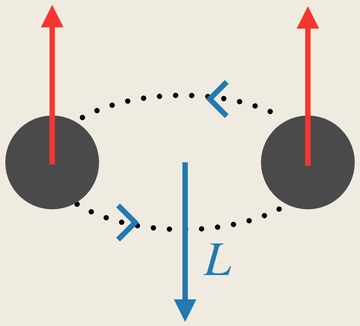

Initial binary

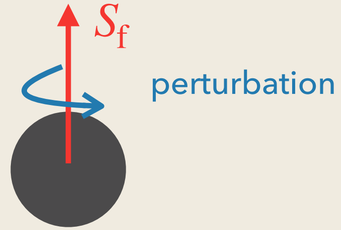

Remnant

Retrograde frequencies excited

Precessing picture

- In precessing systems:
  - Axis of the perturbation is not aligned with the final spin
  - Difficult to quantify the direction of the perturbation

- **Both** prograde **and** retrograde modes are excited

- In co-precessing frame get a “mean frequency”
  $\omega'_{\ell m'} = \omega_{\ell m'} - m'(1 - |\cos\beta|)\left(\omega_{22} - \omega_{21}\right)$

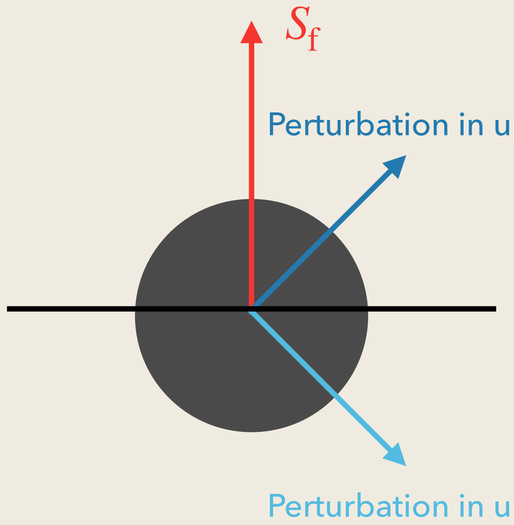

- “positive final spin”
- Prograde frequencies dominate

- “negative final spin”
- Retrograde frequencies dominate

Time domain waveforms

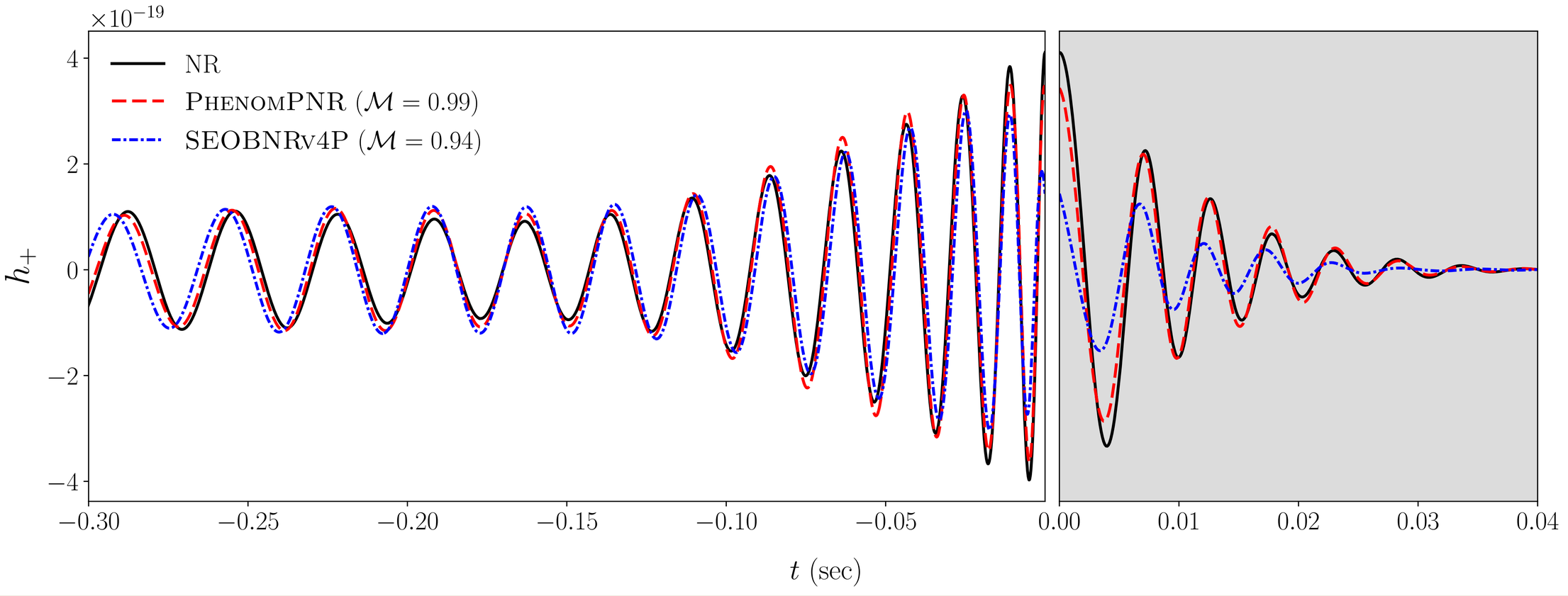

Time domain comparison of

$$q = 8, \chi = 0.8, \theta_{LS} = 60^\circ$$

LISA SCHOOL FOR EARLY CAREER SCIENTISTS – 09.10.25

Current IMR models

MBHB sources

Quasi-circular models

	Modeling approach	Complete inspiral	Calibration (aligned sector)	Calibration (precessing sector)	Extrapolation region
NRSur7dq4	Surrogate	×	$q \leq 4; \lvert\chi_{1,2}\rvert \leq 0.8$	$q \leq 4; \lvert\chi_{1,2}\rvert \leq 0.8$	$q \leq 6; \lvert\chi_{1,2}\rvert \leq 1.0$
PhenomTPHM	Semi-analytic	✓	$q \leq 8; \lvert\chi_{1,2}\rvert \leq 0.8$	×	$q \leq 20; \lvert\chi_{1,2}\rvert \leq 1.00$
PhenomXPHM	Semi-analytic	✓	$q \leq 18; \lvert\chi_{1,2}\rvert \leq 0.95$	×	$q \leq 20; \lvert\chi_{1,2}\rvert \leq 1.00$
PhenomXPNR	Semi-analytic	✓	$q \leq 18; \lvert\chi_{1,2}\rvert \leq 0.95$	$q \leq 8; \lvert\chi_{1,2}\rvert \leq 0.8$	$q \leq 20; \lvert\chi_{1,2}\rvert \leq 1.00$
SEOBNRv5PHM	Semi-analytic	✓	$q \leq 20; \lvert\chi_{1,2}\rvert \leq 0.95$	×	$q \leq 20; \lvert\chi_{1,2}\rvert \leq 1.00$
TEOBResumS-Giotto	Semi-analytic	✓	×	×	–

Modelling challenges: higher modes

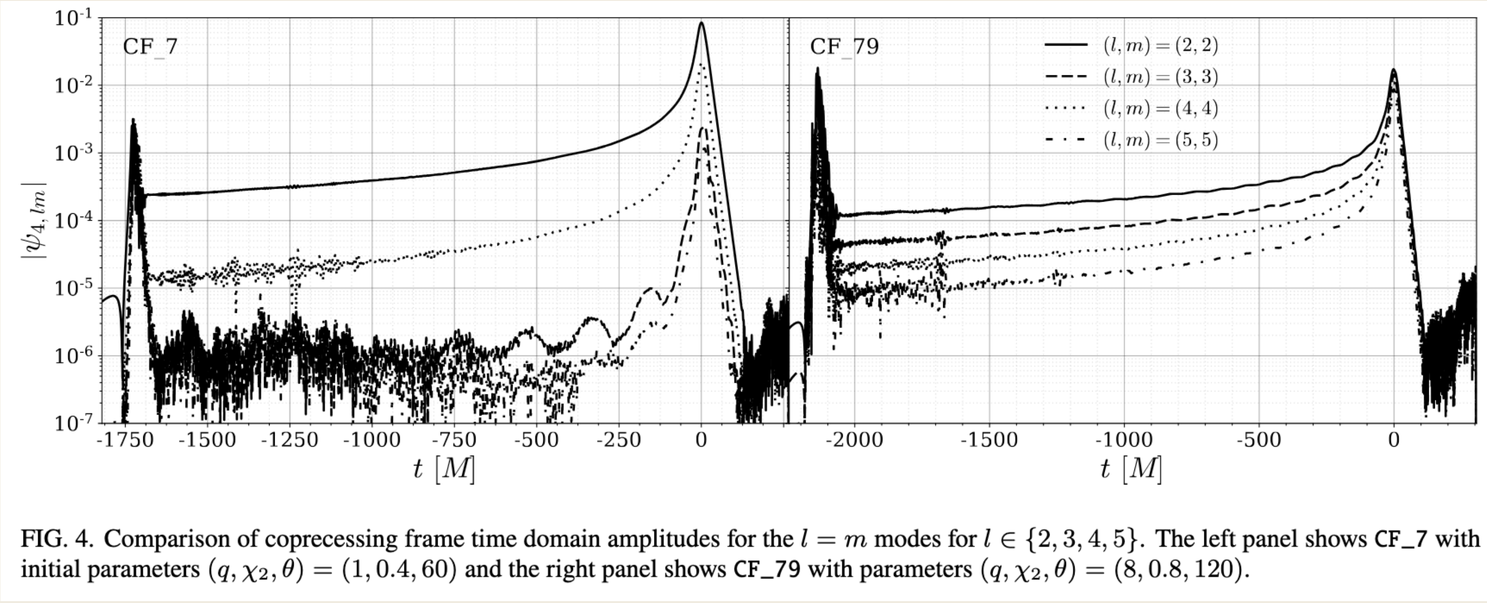

FIG. 4. Comparison of coprecessing frame time domain amplitudes for the $l = m$ modes for $l \in \{2, 3, 4, 5\}$. The left panel shows CF_7 with initial parameters $(q, \chi_2, \theta) = (1, 0.4, 60)$ and the right panel shows CF_79 with parameters $(q, \chi_2, \theta) = (8, 0.8, 120)$.

Hamilton, E., et al. Physical Review D 109.4 (2024): 044032.

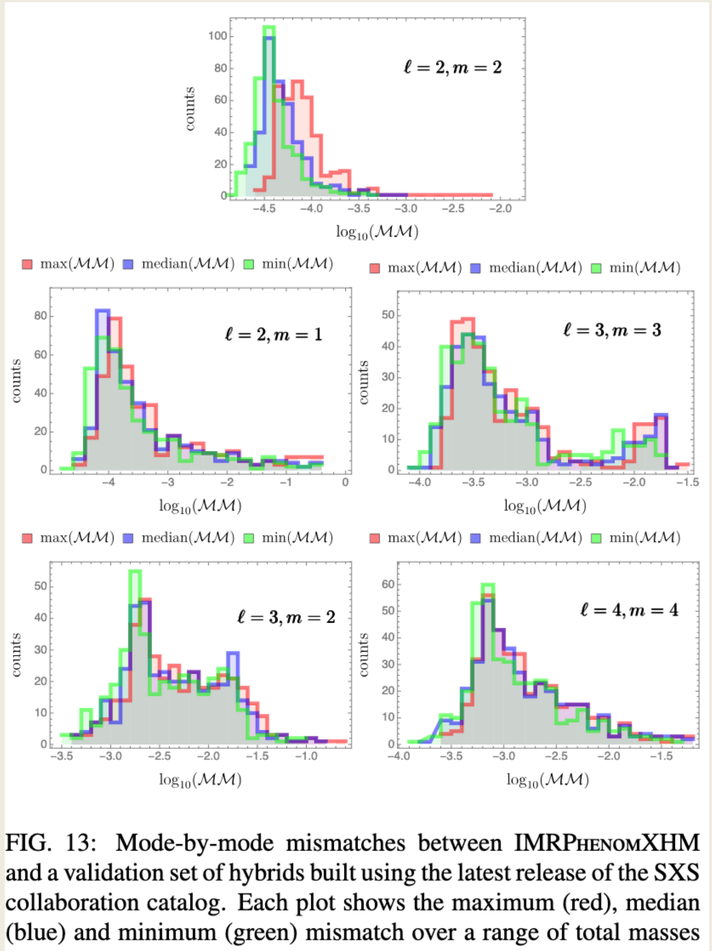

FIG. 13: Mode-by-mode mismatches between IMRPhenomXHM and a validation set of hybrids built using the latest release of the SXS collaboration catalog. Each plot shows the maximum (red), median (blue) and minimum (green) mismatch over a range of total masses

García-Quirós, C., et al. PhysRevD 102.6(2020): 064002.

QC models: model accuracy

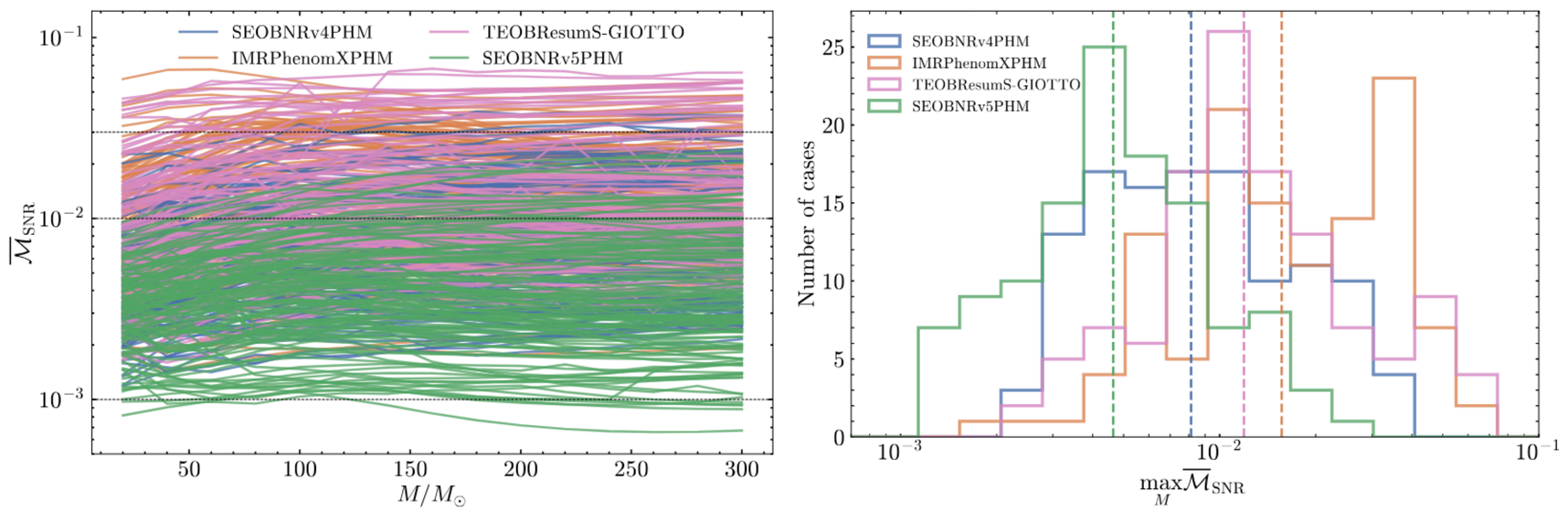

Figure 4. *Left panel:* Sky-and-polarization averaged, SNR-weighted unfaithfulness in the total mass range between $[20-300]M_\odot$ for an inclination $\iota = \pi/3$, between `SEOBNRv4PHM` (blue), `IMRPhenomXPHM` (orange), `TEOBResumS-GIOTTO` (pink) and `SEOBNRv5PHM` (green) against NR for the 118 highly precessing-spin BBH simulations from Ref. [98]. The dashed horizontal vertical lines correspond to the 10^{-3}, 0.01 and 0.03 unfaithfulness values. *Right panel:* Distribution of the maximum unfaithfulness over the total mass range for each NR simulation considered in the left plot. The vertical dashed lines indicate the median values of the distribution.

Ramos-Buades, A., et al. "Next generation of accurate and efficient multipolar precessing-spin effective-one-body waveforms for binary black holes." Physical Review D, 108.12 (2023): 124037.

QC models: parameter recovery

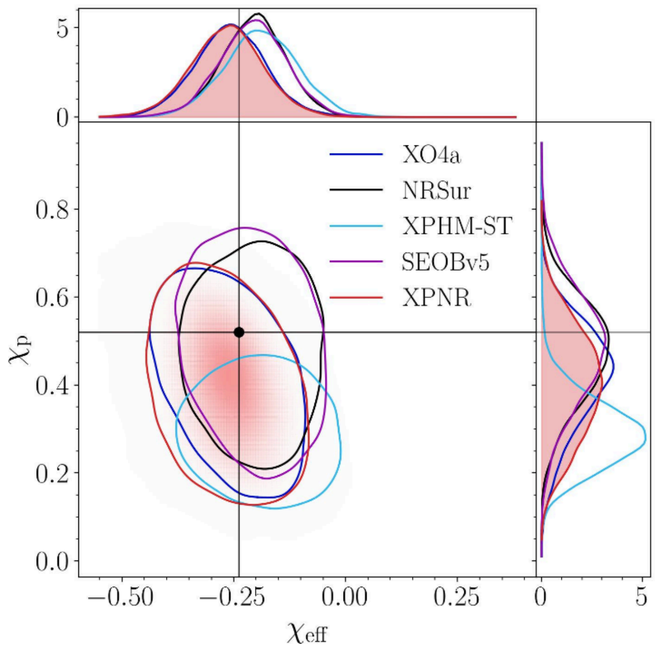

FIG. 11. Comparison between the two-dimensional marginalized posterior distributions for the effective parallel spin χ_{eff} and effective perpendicular spin χ_p when analysing the CF_54 numerical relativity simulation [39]. The contours encase 90% probability. The black crosshairs show the true values.

Hamilton, E., Colleoni, M. et al. arXiv:2507.02604 (2025).

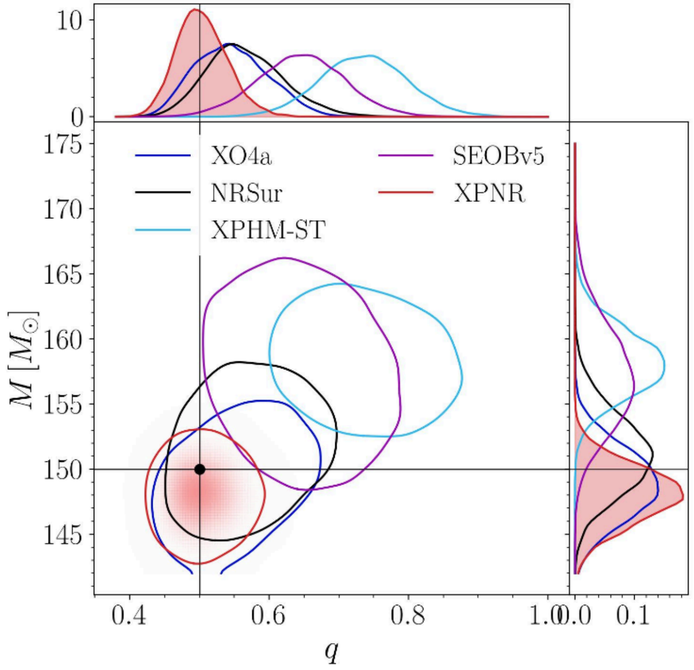

FIG. 12. Comparison between the two-dimensional marginalized posterior distributions for the binary total mass M and mass ratio q when analysing an NRSur7dq4 injection. The contours encase 90% probability. The black cross hairs show the true values.

Hamilton, E., Colleoni, M. et al. arXiv:2507.02604 (2025).

QC models: timing

- Frequency domain models typically most efficient
- Phenom family more efficient
- Adding in additional physics slows down model evaluation

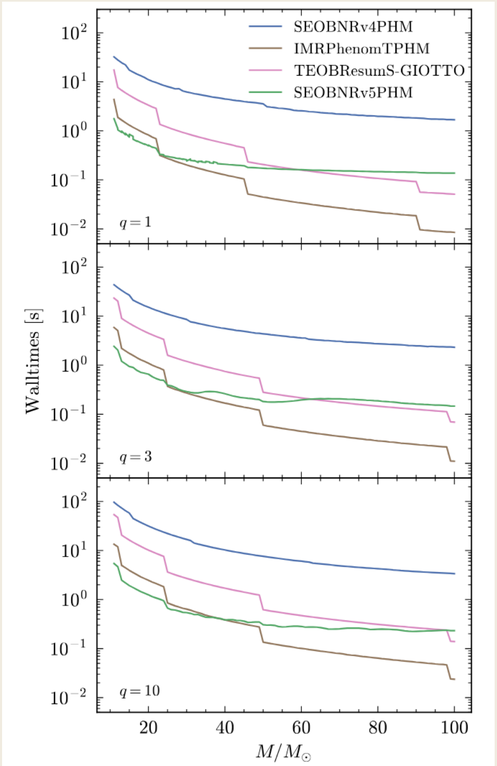

Figure 11. Walltimes of the `SEOBNRv4PHM`, `IMRPhenomTPHM`, `TEOBResumS-GIOTTO` and `SEOBNRv5PHM` models for a configuration with dimensionless spins $\boldsymbol{\chi}_1 = [0.5, 0, 0.8]$, $\boldsymbol{\chi}_2 = [0, 0.5, 0.3]$, total mass range $M \in [10, 100] M_\odot$, starting frequency $f_{\rm start} = 10$Hz and three different mass ratios 1 (top panel), 3 (mid panel) and 10 (bottom panel).

Ramos-Buades, A., et al. (2023). Physical Review D, 108(12), 124037.

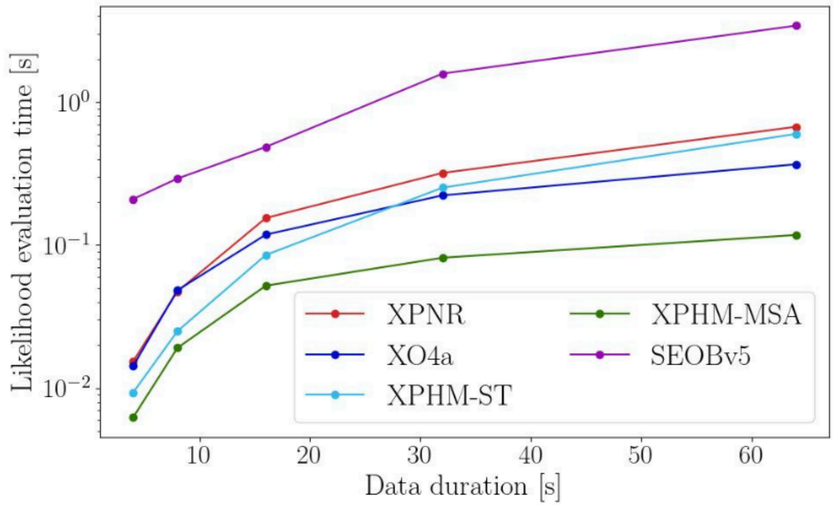

FIG. 16. Comparison between likelihood evaluation times for varying data duration. We compare the evaluation times for four different FD models: PHENOMXPNR, PHENOMXO4A, PHENOMXPHM-SPINTAYLOR, and the TD model: SEOBNRv5PHM. Each data point represents the mean of 10,000 likelihood evaluations calculated via BILBY. Binary parameters were drawn from priors distributions that cut the chirp mass parameter space to ensure that the gravitational waves fit within the specified data duration: larger data durations correspond to smaller chirp mass binaries.

Hamilton, E., Colleoni, M. et al. arXiv:2507.02604 (2025).

Eccentric models

	Modeling approach	Complete inspiral	Calibration to eccentric systems	Precessing extension
NRSurE_q4NoSpin_22	Surrogate	×	$q \leq 1; e \leq 0.25$	×
NRSur2dq1Ecc	Surrogate	×	$q = 1; e \leq 0.2$	×
PhenomTEHM	Semi-analytic	✓	×	×
PhenomXE	Semi-analytic	✓	×	×
SEOBNRv5EHM	Semi-analytic	✓	×	×
TEOBResumS-Dali	Semi-analytic	✓	×	×

Eccentric models: model accuracy

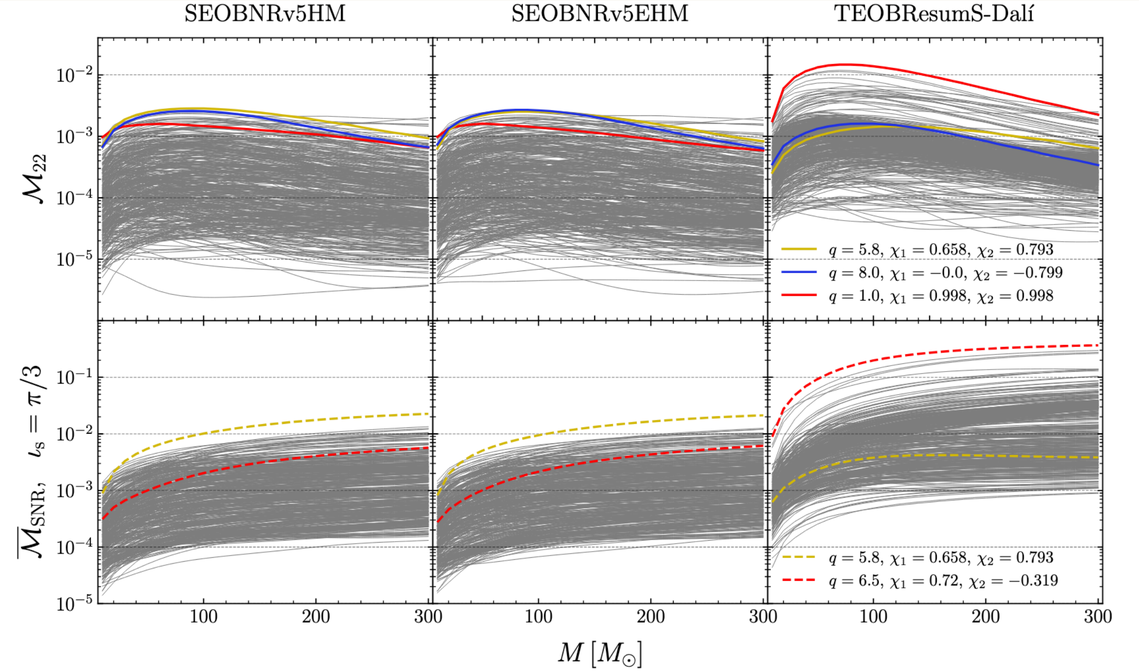

Figure 1. Waveform mismatches between different aligned-spin approximants and the 441 SXS QC NR simulations used in this work, calculated over a range of total masses between 10 and 300 $M_\odot$. The first column corresponds to the QC `SEOBNRv5HM` model, the second column to the eccentric `SEOBNRv5EHM` model, and the third column to the eccentric `TEOBResumS-Dalí` model. The top panels show the $(2,2)$-mode mismatch $\mathcal{M}_{22}$ for each NR waveform, and the bottom panels show the sky-and-polarization averaged, SNR-weighted mismatch $\overline{\mathcal{M}}_{\rm SNR}$ (which takes into consideration higher-order modes) for inclination $\iota_s = \pi/3$. The colored lines highlight cases with the worst maximum mismatch for each model (solid lines for $\mathcal{M}_{22}$ and dashed lines for $\overline{\mathcal{M}}_{\rm SNR}$) with the legends indicating the parameters of the worst-case mismatch for the corresponding model.

Gamboa, Aldo, et al. "Accurate waveforms for eccentric, aligned-spin binary black holes: The multipolar effective-one-body model SEOBNRv5EHM." Physical Review D 112.4 (2025): 044038.

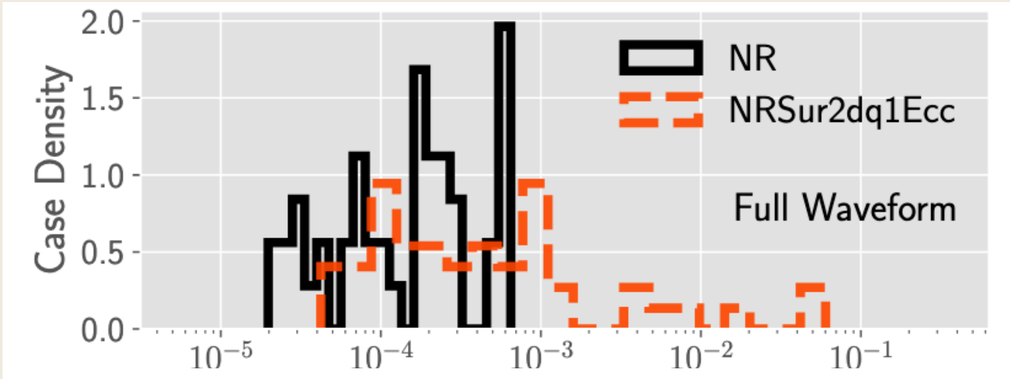

Figure 6. Time-domain leave-one-out errors $\mathcal{E}$, defined in Eq. (17), for the full waveform as well as the individual modes considered in the model. For comparison, we also show the NR error between the two highest resolutions. The largest errors are found near the parameter domain's boundary where the trial surrogate, built as part of the cross-validation study, is extrapolating.

Islam, Tousif, et al. "Eccentric binary black hole surrogate models for the gravitational waveform and remnant properties: Comparable mass, nonspinning case." Physical Review D 103.6 (2021): 064022.

Eccentric models: parameter recovery

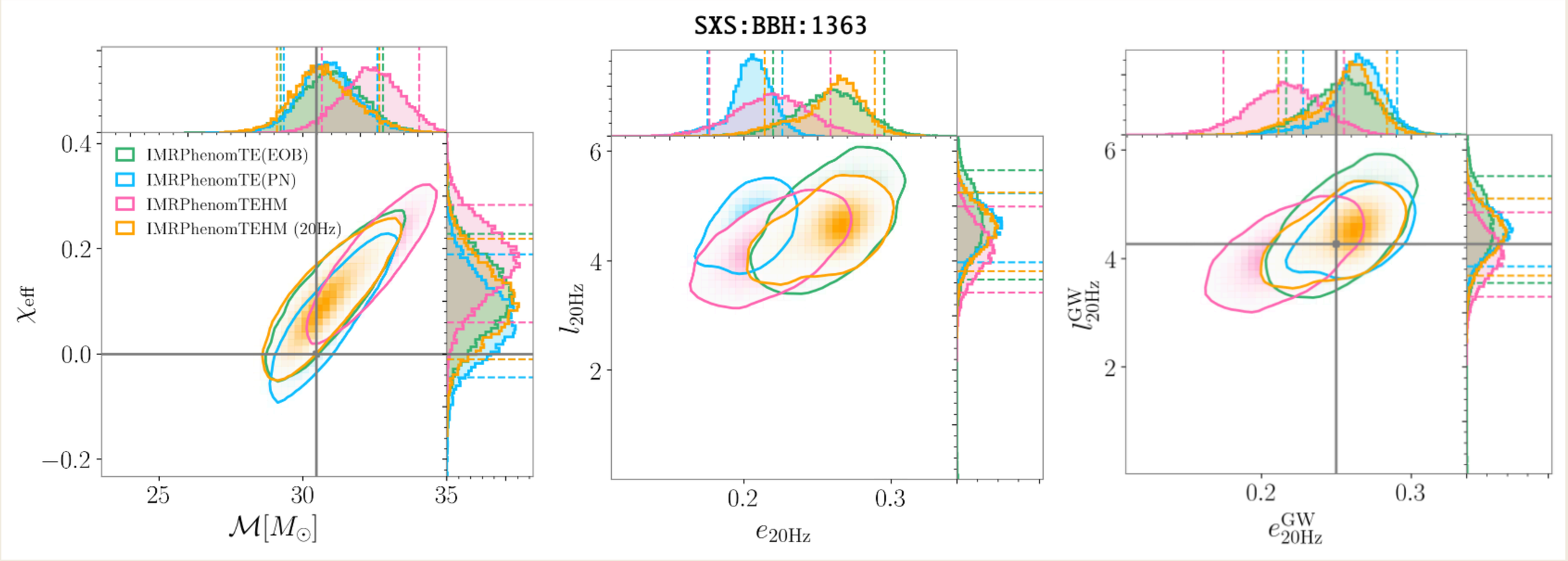

Planas, Maria de Lluc, et al. "Time-domain phenomenological multipolar waveforms for aligned-spin binary black holes in elliptical orbits." arXiv preprint arXiv:2503.13062 (2025).


MINISTERIO
DE CIENCIA, INNOVACIÓN
Y UNIVERSIDADES
Cofinanciado por
la Unión Europea
AGENCIA
ESTATAL DE
INVESTIGACIÓN


LIGO
VIRGO
KAGRA


cost
EUROPEAN COOPERATION
IN SCIENCE & TECHNOLOGY


Finançat per
la Unió Europea
NextGenerationEU
Pla de Recuperació,
Transformació i Resiliència
GOBIERNO
DE ESPAÑA
Conselleria d'Educació
i Universitats
Direcció General d'Universitats, Recerca
i Ensenyaments Artístics Superiors


UIB
Universitat
de les Illes Balears
IAC3
Institut d'Aplicacions
Computacionals
de Codi Comunitari


Conselleria d'Educació
i Universitats
Direcció General d'Universitats, Recerca
i Ensenyaments Artístics Superiors


Illes
Sostenibles
Impost de Turisme Sostenible


REDONGRA
Red Española de Física de Ondas Gravitacionales
Spanish Network of Gravitational Wave Physics


Cofinanciado por
la Unión Europea
Cofinançat per
la Unió Europea


MINISTERIO
DE HACIENDA


Fondos Europeos
Fons Europeus


Govern de les
Illes Balears
Conselleria d'Educació
i Universitats


Cofinanciado por
la Unión Europea
Cofinançat per
la Unió Europea


MINISTERIO
DE TRABAJO
Y ECONOMÍA SOCIAL


Fondos Europeos
Fons Europeus


Govern de les
Illes Balears
Conselleria d'Educació
i Universitats